UPTEC X11 048
Examensarbete 30 hp
Januari 2012

The oligomeric structure of Poly(A)-specific ribonuclease (PARN)

Mikael Nissbeck

UPPSALA UNIVERSITET

Molecular Biotechnology Programme

Uppsala University School of Engineering

UPTEC X11 048	**Date of issue 2012-01**

Author

Mikael Nissbeck

Title (English)

The oligomeric structure of Poly(A)-specific ribonuclease (PARN)

Title (Swedish)

Abstract

Poly(A)-specific ribonuclease (PARN) is a deadenylase that degrades the poly(A) tail of eukaryotic mRNA. PARN also interacts with the 5'-cap structure of the mRNA. The binding of the cap structure enhances the deadenylation rate. PARN has previously been described as a dimer. We have studied PARN with size exclusion chromatography to investigate the oligomeric composition and revealed oligomeric compositions of PARN that are larger than dimeric PARN. Deadenylation assays have been used to measure the cap stimulated activity of PARN. The deadenylation assays showed that the cap stimulated activity of PARN correlated with the abundance of oligomers corresponding in size to tetrameric PARN. We present a model for tetrameric PARN and propose a mechanistic model for how the cap stimulates PARN mediated deadenylation.

Keywords

Poly(A)-specific ribonuclease (PARN), deadenylation, mRNA metabolism, cap stimulation, oligomerization.

Supervisors

Anders Virtanen
ICM, Uppsala University

Scientific reviewer

Torsten Unge
ICM, Uppsala University

Project name	Sponsors
Language **English**	Security
ISSN 1401-2138	Classification
	Pages **31**

Biology Education Centre Biomedical Center Husargatan 3 Uppsala
Box 592 S-75124 Uppsala Tel +46 (0)18 4710000 Fax +46 (0)18 471 4687

Determining the oligomeric structure of PARN

Mikael Nissbeck

Populärvetenskaplig sammanfattning

Informationen i våra celler skickas från DNAt i kärnan till ribosomen via mRNA. Två element sätts på mRNA, en så kallad ”cap” i början och en poly(A)-svans i slutet av mRNAt. Båda dessa strukturer skyddar mRNAt från degradering. Enzymet poly(A)-specific ribonuclease (PARN) degraderar poly(A)-svansen. Detta innebär att PARN är ett viktigt enzym för mRNA-regleringen i våra celler. Ett unikt inslag hos PARN är att ”cap” strukturen hos mRNAt ökar degraderingshastigheten av poly(A)-svansen. PARN har visats bilda en dimer men det finns även antydningar att PARN kan förekomma som en tetramer.

Projektet går ut på att visa att en PARN-tetramer existerar och att undersöka om den ”cap”-stimulerade poly(A)-degraderingsaktiviteten är resultat av tetramerisering eller om denna effekt återfinns hos dimer och monomer. Mutationer har införts i PARN för att undersöka vilka aminosyror som är viktiga för tetramerisering av PARN. För att visa tetramerisering av PARN har två metoder använts, storleksfraktionering och korsbindning av PARN. Degraderingsförsök har gjorts med ”cappat” och ”ocappat” mRNA, för att demonstrera ”cap”-stimuleringen.

De försök som har gjorts demonstrerar att PARN är en potentiell tetramer. Vi har även visat att både ”cap”-stimuleringen och tetrameriseringen förändras i olika saltkoncentrationer. Sammantaget visar studien att ”cap”-stimuleringen har sitt ursprung i PARN tetrameren.

Examensarbete 30 hp

Civilingenjörsprogrammet Molekylär Bioteknik

Uppsala Universitet, januari 2012

Table of contents

1 Introduction

1.1 mRNA metabolism

The central dogma of life describes the flow of information in the cells, from DNA to RNA and from RNA to protein. The flow of information starts in the genome where the DNA is transcribed into a single stranded RNA called pre-messenger RNA (pre-mRNA) by RNA polymerase II. The pre-mRNA is processed during transcription. The coding exons are joined together by the spliceosome and the ends of the pre-mRNA are modified with two elements that are added during and after transcription. At the 5'-end a guanine, methylated at position seven, is added to form the 5'-cap structure (m^7GpppG) and at the 3'-end a tail of adenines that forms the poly(A) tail is added.

The capping of the mRNA occurs after 20-30 nucleotides have been transcribed by RNA polymerase II. After capping of the nascent pre-mRNA the RNA polymerase II continues transcribing the gene (Proudfoot et al., 2002). The cap is added in two steps; first a guanine-tri-phosphate is added to the tri-phosphate of the first transcribed nucleotide of the mRNA by guanyl transferas, followed by methylation of the nitrogen at the seventh position of the guanine purine ring (Proudfoot et al., 2002). The last element to be added to the pre-mRNA is the poly(A) tail, which is added by a process called nuclear polyadenylation, a process that first cleaves the pre-mRNA and then synthesizes a 200 nucleotide long adenosine tail at the 3' end of the cleaved pre-mRNA. The polyadenylation machinery is composed of approximately 13 different proteins (all together one mega-Dalton in molecular weight) in mammalian cells and it includes a site specific endoribonulcease activity as well as the essential poly(A) polymerase (PAP) (Mandel et al., 2008). Sequence elements in the 3' untranslated region (UTR) of the pre-mRNA are important for positioning the cleavage and polyadenylation complex to the polyadenylation site. Upstream of the cleavage and polyadenylation site are two sequence elements; a U-rich sequence region and the polyadenylation signal sequence AAUAAA. Also downstream elements, including a G/U-rich element, are used to stabilize the pre-mRNA before cleavage (Mandel et al., 2008). The cleavage and polyadenylation complex include; the cleavage and specificity factor (CPSF), two cleavage factors (CFI and CFII), cleavage stimulation factor (CstF) and two proteins, PAP and symplekin (Zhang et al., 2010). Efficient polyadenylation requires the nuclear poly(A) binding protein (PABPN1), and each PABPN1 binds to 11-14 adenosines. Binding of PABPN1 to newly synthesized poly(A) tail stimulates PAP to add the 200-300 nt long poly(A) tail (Mandel et al., 2008). The interaction between PABP and the poly(A) tail protects the mRNA from deadenylase activity (Gorgoni and Gray, 2004). The mature mRNA contains and carries the genetic information from the nucleus to the cytoplasm (Proudfoot et al., 2002).

The eukaryotic mRNA contains five parts; the amino acid sequence blueprint of the protein, *i.e.* the open reading frame (ORF), the 5' and 3' UTRs that flank the ORF, a 5'-cap and the 3'-end poly(A) tail. The 5'UTR harbors the ribosome binding site (RBS) and in the 3'UTR different regulatory sequences are found that regulate deadenylation or re-

polyadenylation (Zhang et al., 2010). Before translation the mRNA is circularized by initiation factors 4E (eIF4E), eIF4G and cytoplasmic poly(A) binding protein (PABP). eIF4E is the cytoplasmic cap binder that binds the cap of the mRNA and PABP binds the poly(A) tail in the cytoplasm. Both eIF4E and PABP interacts with eIF4G, and together they circularize the mRNA (Wells et al., 1998). The circularization of the mRNA enhances the translation. Both the cap and the poly(A) tail affect the stability the mRNA and acts as "hooks" for transport out of the nucleus.

1.2 mRNA degradation

The genome is regulated by various transcription factors that bind to the DNA and activate the transcription of the gene (Halbeisen et al., 2007). The transcribed RNA constitutes the inflow of information to the transcriptome. The transcriptome is being regulated by the inflow and degradation of the RNAs.

mRNA turn-over utilizes four characteristic enzymatic reactions; decapping, 3'-5'-exonucleolytic degradation, 5'-3'- exonucleolytic degradation and endonucleolytic cleavage of the mRNA. The mRNA metabolism can be divided in two main degradation mechanisms, unspecific or sequence-specific degradation of mRNA. In sequence-specific mRNA degradation microRNA (miRNA) base pairs with a sequence in the 3'UTR of the mRNA, to form a dsRNA region. The dsRNA is then cleaved by an endonuclease activity and the two mRNA halves are subsequently degraded. The miRNA can also recruit proteins that build up the miRNA induced silencing complex (miRISC), which may induce degradation of the mRNA (Tang, 2005). The unspecific degradation of mRNA occurs in one of the three different mRNA decay pathways; i) deadenylation-dependent mRNA decay, ii) deadenylation-independent mRNA degradation and iii) endonuclease-mediated mRNA degradation (Parker and Song, 2004).

1.2.1 Deadenylation-dependent mRNA decay

Deadenylation-dependent mRNA decay begins with the removal of the poly(A) tail (deadenylation) by a deadenylase activity. Three major deadenylases have been identified in mammalian cells, poly(A) nuclease (PAN), poly(A)-specific ribonuclease (PARN) and the CCR4/CAF1/NOT deadenylation complex. Deadenylation of the poly(A) tail is the rate limiting step in mRNA degradation (Goldstrohm and Wickens, 2008). Deadenylation is either followed by the removal of the 5'-cap by decapping protein 2 (DCP2) and subsequent degradation of the mRNA body the 5'-3'-exoribonuclease XRN1 or by 3'-5' degradation of the deadenylated mRNA by the exosome. The exosome degrades the mRNA up to the first transcribed base after the cap, which finally is degraded by scavenger decapping protein (DcpS).

Deadenylases depend on Mg^{2+} for their ability to catalyze the cleavage of poly(A) tail phosphate-backbone and this reaction results in release of free 5'-AMP (Goldstrohm and Wickens, 2008, Garneau et al., 2007). The deadenylases belong to the DEDD super family of nucleases or the exonuclease-endonuclease-phosphatase (EEP) super family. Deadenylases that belongs to the DEDD super family have an active site consisting of the

four conserved acidic amino acids, three Asp (D) and one Glu (E) that coordinate the two divalent metal ions in the active site. Deadenylases belonging to the DEDD super family are POP2, CAF1Z, PARN and PAN2. Deadenylases belonging to the EEP super family are CCR4, nocturnin, ANGEL and 2' phosphodiesterase (2'PDE) (Goldstrohm and Wickens, 2008).

1.2.2 Deadenylation-independent and endonuclease-mediated mRNA decay

The majority of the degraded mRNA goes through the deadenylation-dependent mRNA decay pathway, but there are two alternative pathways of mRNA decay independent of deadenylation (Parker and Song, 2004). In deadenylase-independent mRNA decay the 5'-cap is first removed by Dcp2 and then the mRNA is degraded by the 5'-3'-exonuclease XRN1. The third pathway of mRNA decay is mediated by an endonuclease that cleaves the mRNA into two half's, the poly(A) half and 5'-cap half. The poly(A) half is degraded in the 5'-3' direction by XRN1 and the 5'cap half is degraded by the exosome followed by scavenger decapping. (Garneau et al., 2007)

1.3 PARN

The majority of eukaryotic mRNA degradation starts by the deadenylation of the poly(A) tail (Goldstrohm and Wickens, 2008). PARN is an exoribonuclease with high specificity for poly(A) and acts by stepwise shortening of the poly(A) tail in the 3'-5' direction (Åström et al., 1992, Körner et al., 1998, Henriksson et al., 2010). PARN is localized both in the nucleus and the cytoplasm (Körner et al., 1998). In the nucleus PARN is inhibited by the cap binding complex (CBC) (Balatsos et al., 2006). The 3'-5' exoribonuclease activity of PARN, when acting on poly(A) tails releases free 5'-AMP mononucleotides (Åström et al., 1992, Martínez et al., 2000). PARN is the only known deadenylase to interact with the 5'-cap structure of the mRNA while degrading the poly(A) tail (Gao et al., 2000, Martínez et al., 2000, 2001). The cap interaction enhances the processivity of deadenylation, i.e. the cap structure is an allosteric activator (Martínez et al., 2001). Increased processivity means that PARN shortens the poly(A) tail faster before releasing the mRNA body. In *in vitro* experiments it has been observed that a cap stimulatory effect on uncapped substrates is induced by the addition of a low concentration of free cap analogue whereas the addition of a high concentration of the cap analogue inhibits PARN activity (Martínez et al., 2001). The activity of PARN is also inhibited if there are secondary structures in the beginning of the 5'-UTR (Gao et al., 2000).

PARN has three structural domains; the nuclease domain and two RNA binding domains, i.e. the RNA recognition motif (RRM) and the R3H (Wu et al., 2005, 2009). The C-terminal extension of PARN is known to interact with both the cap binding complex (CBC) (Balatsos et al., 2005) and cleavage stimulation factor (CstF) in the cleavage and polyadenylation machinery (Cevher et al., 2009). CBC has two subunits, CBP-20 and CBP-80, the small subunit interacts with the cap and the large subunit interacts with PARN and inhibits the deadenylation activity of PARN (Balatsos et al., 2005). In contrast, the interaction of PARN with CstF activates PARN activity (Cevher et al., 2009).

In the three crystal structures that have been solved (i.e. PARN in the absence of poly(A), in complex with poly(A) and in complex with cap) PARN forms a homodimeric structure (Wu et al., 2005 and 2009). The nuclease dimerization interactions are created by two α-helices and one β-strand from each monomer (Wu et al., 2005). When mutations were introduced to disrupt the nuclease-nuclease-dimerization, the resulting monomer had no deadenylation activity and it was speculated that the dimer formation was required to stabilize the active site (Wu et al., 2005).

The active site of PARN consists of four acidic amino acids dispersed on three sequence motifs; ExoI harbors Asp-28 and Glu-30 while Asp-292 and Asp-382 belong to the ExoII and ExoIII motifs, respectively (Ren et al., 2002). The sequence motifs of ExoI-III fold into the DEDD active site. The amino acids Asp-28, Glu-30 and Asp-382 are in direct contact with divalent metal ions while the metal ion connection between Asp-292 and the divalent metal ion is bridged by one water molecule (Ren et al., 2002). The deadenylase activity of PARN requires divalent (Mg^{2+} or Mn^{2+}) and monovalent (Na^{+} or K^{+}) ions. The highest activity is gained when potassium and magnesium ions are used in the reaction (Åström et al., 1992 and Liu et al., 2009). If the Asp residues in the active site are substituted with Cys the resulting mutants are inactive in the presences of Mg^{2+} but regain the activity in the presence Mn^{2+} (Ren et al., 2004). The negatively charged amino acids coordinate the metal ions and the metal ions coordinate the phosphodiester bond between the adenine nucleotides in the poly(A) tail (Ren et al., 2004). For PARN to perform catalysis, one histidine is essential in the hydrolysis reaction (Wu et al., 2005).

PARN contains two RNA binding domains, the RRM and the R3H. The R3H stabilizes the RNA during degradation (Liu et al., 2007) whereas the RRM interacts with the substrate and binds the 5'-cap of the mRNA (Nilsson et al., 2007). The interaction between PARN and the cap occurs at the interface between the active site and the RRM (Nilsson et al., 2007). The 7-methyl guanine stacks against Trp-475 in the RRM and the first transcribed guanine is coordinated by amino acids near the active site. The cap interaction rotates the RRM to the nuclease domain, and the RRM is placed in a so called closed conformation (Wu et al., 2009). The RRM has two conformational states, open or closed, and the rotation angle of the RRM from the open to closed is 30˚ (Wu et al., 2009). The cap interacts with both the RRM and the active site; this interaction increases the processivity of PARN (Martínez et al., 2001). Thus, the cap is an allosteric activator for the PARN deadenylation activity (Wu et al., 2009). Neither of the RRM or the R3H domains are necessary for the deadenylation activity of PARN. However, the presence of the two RNA binding domains stabilizes the substrate and increase PARN activity (Liu et al., 2007). The RRM is involved in binding of the substrate and to feed the poly(A) substrate into the active site (Henriksson et al., 2010). Furthermore, the RRM has been shown to form a homodimer when fractionated by size exclusion chromatography (SEC) (Niedzwiecka et al., 2011).

Native PARN has a six-fold higher deadenylation rate on capped mRNA substrate than recombinant PARN. The molecular reason for this difference in activity is not yet

understood. One reason for the difference in activity between native and recombinant PARN could be due to differences in oligomeric arrangement. PARN was shown to form a dimer in the crystal (Wu *et al,.* 2005). On the other hand, in the crystal packing of PARN (pdb 3D45), PARN was organized as tetramers (not published). The crystal packing indicates a potential tetramerization between two PARN dimers. The tetramerization surface was located in the RRM domains. From the crystal packing the amino acid Leu-464, Ile-493, Thr-497, Tyr-500 and Tyr-504 were identified in the tetramerization surface between the two PARN dimers. The aim of this study was to investigate the oligomeric arrangement of PARN and the cap stimulation of the deadenylation activity.

2 Materials and methods

2.1 Mutagenesis

Human PARN was originally cloned into the IPTG (isopropyl β-D-1-thiogalactopyranoside) inducible expression plasmid pET33(+) (Nilsson and Virtanen, 2005). PCR mutagenesis was performed according to Stratagene QuikChange ® Site-Directed Mutagenesis protocol (Stratagene). PCR mutagenesis primers were designed to introduce alanine in the desired position by changing the native to the alanine codon (Table 1). The PCR reaction contained 2.5 U pfuTurbo with supplied buffer (Stratagene), 25 mM of each nucleotide (ATP, GTP, TTP and CTP), 125 ng of each forwarded and reverse primer and 5 % DMSO. The total PCR reaction volume was 50 µl. The reaction was performed in 4 steps; the first step was an initial denaturation in 95˚C for 10 minutes. Two cycle steps with denaturation (95˚C, 30 seconds), annealing (60˚C and 55˚C, 1 minute) and elongation (68˚C, 8 minutes), the cycle with the high annealing temperature was repeated three times while the low annealing temperature was repeated 15 times. The last step in the PCR program was a 20 minute long extra elongation step. After the PCR the template was digested with Dpn1 (Stratagene) followed by precipitation of the PCR product. Precipitation of the Dnp1 treated PCR product by adding 3xPCR volume 99.5% ethanol and 1/10 PCR volume 3M sodium acetate at pH 5.2 and incubated in -20˚C for 2 h. The precipitated PCR product was pelleted at 13000 rpm for 15 minutes at 4˚C, the formed pellet was washed with 1 ml 70% ethanol and recovered as in the previous step. The pellet was dried and resuspended in 5 µl H_2O. 1 µl was used to transform 15 µl One Shot competent TOP10 cells (Stratagene). The transformed cells were grown on LA-plates with 50 µg/ml kanamycin. Clones from the plate were isolated and the plasmids were purified with PureYield™ Plasmid Miniprep System (Promega, #A1222). The introduced mutation was verified by sequencing of the isolated plasmids.

Table 1. Primer design for the insertion of mutation in PARN, bold letters shows where the native codon was change to an alanine codon.

Primer	Sequence
Y500A_Y504A_F	5'- C AAT ACC AGC AAA **GC**T GCA GAA AGC **GC**T CGG ATC CAA AC -3'
T500A_Y504A_R	5'- GT TTG GAT CCG A**GC** GCT TTC TGC A**GC** TTT GCT GGT ATT G -3'

2.2 Expression and purification

The expression and purification of PARN was performed according to Nilsson and Virtanen (Nilsson and Virtanen, 2005) and summarized below.

His-tagged wild type PARN and PARN construct plasmids were transformed into BL-21 (DE3) cells and grown overnight on LA plates at 37˚C with 50 µg/ml kanamycin. Colonies from the plate were used to inoculate 200 ml TB (terrific broth) medium supplemented with 50 µg/ml kanamycin, and incubated in 37˚C overnight under constant rotation (~100 rpm). The 200 ml overnight culture was used to inoculate 1400

ml TB medium supplemented with 50 µg/ml kanamycin. When OD_{600} reached ~0.8-0.9 the expression was induced with 1 mM IPTG (isopropyl-1-thio-β-D-galactopyranoside) final concentration and further incubated for 3 h at 37˚C, followed by harvest of the cells by centrifugation.

The purification of his-tagged PARN and mutants began by resuspending the harvested cell pellet in 8.33 ml extraction buffer (500 mM KCl, 10 % glycerol, 20 mM HEPES pH 7.9, 0.5 % NP-40, 2 mM β-mercaptoethanol and 2.5 mM imidazole) per liter cell culture. The cells where disrupted by sonication and the cell lysate clarified by centrifugation at 19000 rpm (Sorwall SS-34) for 20 minutes in 4˚C. The supernatant was added to 41.7 µl Talon metal affinity resin (Clontech) per liter culture. The Talon resin was washed three times with 10 ml wash buffer (500 mM KCl, 10 % glycerol, 20 mM HEPES pH 7.9, 0.5 % NP-40 and 5 mM imidazole). The his-tagged protein was eluted with 3 ml elution buffer (500 mM KCl, 10 % glycerol, 20 mM HEPES pH 7.9, 0.5 % NP-40 and 250 mM imidazole) and fractions of 0.5 ml were collected. The fractions were analyzed on SDS-PAGE 10% separation gel (29:1 acrylamide/bisacrylamide) and the gel was stained with Comassie R250 blue. The fraction containing most protein was dialyzed over night into 200 mM NaCl and 100 mM KH_2PO_4/K_2HPO_4 pH 7.0 followed by concentration determination according to Bradford (Biorad).

2.3 Size exclusion chromatography fractionation

The full length PARN was fractionated with (SEC) on a SMART fractionation system (Pharmacia/GE Healthcare) using a Superdex™ 200 PC3.2/20 column (GE Healthcare), gel volume 2.4 ml. 20 µl aliquots of PARN were centrifuged at 13000 rpm at 30 minutes in 4˚C prior to loading a 20 µl loop on the SEC-fractionation system. Before the sample fractionation the column was equilibrated with 5 ml of SEC-buffer (50 mM KH_2PO_4/K_2HPO_4 pH 7.0 and 25-200 mM NaCl). Fractions of 20 or 35 µl were collected and frozen in -70˚C.

2.4 Cross linking

Protein-protein cross-linking reaction was performed in 10 mM bis(sulfosuccinimidyl) suberate (BS^3) and purified PARN or PARN mutants. The reaction was performed in room temperature for 5 minutes in a total reaction volume of 30 µl. The reaction contained 10 µM of either PARN or PARN mutants. The reaction was stopped by adding 2µl 1 M Tris-HCl pH 7.0. 10µl of the reaction volume was loaded on a SDS-PAGE gel with a 4% stacking and 5% separation polyacrylamide gel (29:1 acrylamide/bisacrylamide). The "bands" were visualized with both silver staining and Western blot with anti PARN antibodies.

2.5 *In vitro* transcription

The RNA substrate L3(A_{30}) was *in vitro* transcribed from the *Nsi*I cleaved plasmid pT3L3(A_{30}). *In vitro* transcription was made with 100 u T3 RNA polymerase (Strategene, #0006038405), 2 µg of linearized pT3L3(A_{30}), 40 u RiboLock™ RNase Inhibitor (Fermentas, #E00382), 25 mM DTT, 1.33 mM ATP, 0.67 mM GTP, UTP, CTP, 50 mM NaCl

and 40 Ci/mmol [αP^{32}] –ATP in 30 µl reaction. For capping of the substrate 3.33 mM Cap analogue (m^7GpppG) was added to the reaction. The transcription mixture was incubated for 1 h at 37˚C followed by PAGE purification on a 10 % denaturating polyacrylamide gel (19:1 acrylamide/bisacrylamide) containing 7 M urea and run at 10 W for 1 h. The gel was exposed on Amersham Hyperfilm™ ECL (GE Healthcare) and the band containing the substrate was isolated and eluted in water with RNA inhibitor over night at 4˚C. The eluted material was precipitated by adding three times volumes of 99.5% ethanol and one tenth of the volume with 3M NaCl and incubated on ice for 1 h. The pellet was dissolved in water and the concentration of the substrate was determined by counting the radioactive decay in a Scintillator.

2.6 *In vitro* deadenylation

Deadenylation was performed in a total volume of 10 µl containing 50 mM KH_2PO_4/K_2HPO_4 pH 7.0, 50-450 mM NaCl, 2 mM MgCl, 0.1 g/l BSA, 1 unit of RNase inhibitor and 10 nM capped or uncapped L3(A_{30}) to which 0-128 nM PARN was added to the total reaction volume of 10 µl. The reaction was incubated at 30˚C for 10 min and stopped by adding 2 µl of 0.5 M EDTA. 1 µl of the reaction was spotted 1.5 centimeter from the edge of a TLC PEI Cellulose F (Merck). The filter was placed in a 1 centimeter deep reservoir of 0.4 M KH_2PO_4 pH 4, until the buffer migrated to the top of the TLC plate. The TLC plate was dried and exposed to a phosphor imager screen. The phosphor imager screen was analyzed with a Phosphor imager (Molecular dynamics).

3 Results

3.1 Cloning and purification of PARN

To investigate the involvement of the two tyrosine residues, Y500 and Y504, in tetramerization of PARN the residues where mutated to alanines. The mutagenesis was made according to Stratagene QuikChange ® Site-Directed Mutagenesis protocol with primers introducing alanine mutations at both tyrosine locations in the PARN gene. In the first attempt, which was unsuccessful, I followed the Stratagene QuikChange ® Site-Directed Mutagenesis protocol and the obtained PCR products were transformed into competent TOP10 cells. In the second attempt 5% DMSO was added to the PCR reaction and the annealing temperature was raised to 60˚C for three cycles.

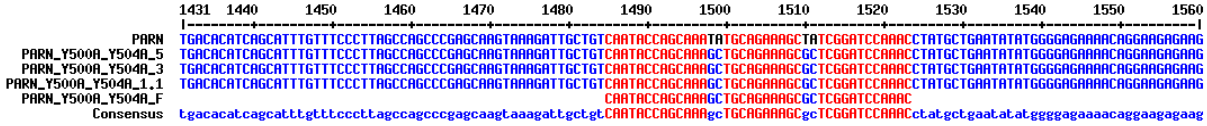

Figure 1. The sequences covering the introduced mutations in the PARN gene for the mutants Y500A Y504A clone 1.1, 3 and 5. The determined sequence of each obtained plasmid has been aligned with the wild type PARN sequence and the forward primer sequence used in the PCR reaction. The codon for Trp, TAT, has been mutated to the codon for Ala, GCT.

In this case colonies appeared on the plate after transformation. The transformation was first made with one fifth of the obtained PCR reaction and resulted in one colony (fig. 1 PARN_Y500A_Y504A_1.1). The second round of transformation was made with four fifth of the obtained PCR reaction and gave rise to five colonies. In total six colonies were isolated and the plasmid DNA was extracted from each of the colonies. The nucleotide sequences of the purified plasmids were subsequently determined (fig 1) and the obtained sequences of each plasmid were compared to the PARN sequence. The sequencing showed that colonies 1.1, 3 and 5 had the two tyrosines residues mutated to alanine (fig 1). The construct that showed no sequencing result was not investigated any further.

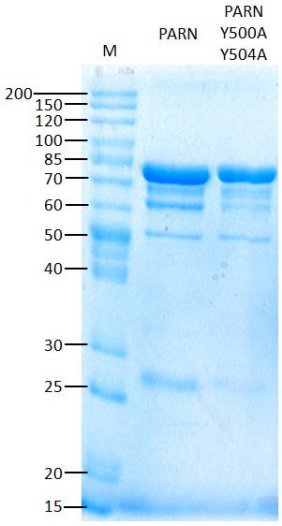

Figure 2. SDS-PAGE separation of PARN and the double tyrosine mutant. The purity of the two PARN types was estimated to be around 95%.

The expression and purification of mutant and wild type PARN polypeptides were performed according to Nilsson and Virtanen (Nilsson and Virtanen, 2005). The plasmids for wild type PARN and the double tyrosine mutant (PARNY500,504A) were transformed into BL-21 (DE3) cells. The cells where harvested by centrifugation and the pellet was resuspended in extraction buffer and the cells disrupted by sonication. The resulting total lysate was clarified by centrifugation and the supernatant was added to Talon resin that has high affinity and specificity for binding his-tagged proteins. After washing the Talon resin with wash buffer the protein was eluted form the Talon resin by the addition of high concentrations of imidazole that competes out the his-tagged protein from the resin. Fraction 1 was dialyzed over

night against 200 mM NaCl and 100 mM KH_2PO_4/K_2HPO_4 pH 7.0. The protein concentration of the dialyzed PARN fraction was determined by using Bradford and comparing the absorbance of the purified protein fraction against a known reference protein concentration. After purification a purified PARN fraction of a concentration of 1.87 g/l was obtained, which corresponds to 25.2 μM. The purification of double tyrosine mutants resulted in purified fraction containing 0.82 g/l mutant PARN corresponding to 11.07 μM. The purity was estimated to be approximately 95% (fig 2).

3.2 The oligomeric structure

The three crystal structures of PARN (pdb codes: 2A1S, 2A1R and 3D45) reveal PARN as a homodimer, with a dimerization surface between the two nuclease domains (Wu et al., 2005 and 2009). Interestingly, a recent study has revealed that the RRM of PARN forms dimers (Niedzwiecka et al., 2011). Furthermore, it has been observed that native PARN purified from calf thymus has deadenylation activity in purified fractions with an apparent higher molecular weight larger than the estimated weight of a dimer (Martínez et al., 2000).

To investigate the oligomeric composition of recombinant PARN expressed and purified from E. coli, we used the SEC-fractionation system with a SuperdexTM 200 PC3.2/20 column and BS3 cross-linking. SEC- fractionation is a common method for separation of proteins and protein complexes by their size, and it has frequently been used to characterize large protein assemblies, for example the two mega-Dalton complexes of the CCR4/CAF1/NOT deadenylase (Denis and Chen, 2003). An approach to investigate protein-protein interactions in large protein assemblies is to use chemical cross-linkers, which form covalent bonds between interacting proteins.

We used bis(sulfosuccinimidyl) (BS^3) to cross-link purified PARN and size separation with SDS-PAGE. Detection of the cross-linked oligomers of PARN was done with silver staining and Western blotting, using antibodies against PARN. The use of Western blot analysis will confirm that the detected oligomers contain PARN.

The purified recombinant PARN used during SEC-fractionation and cross-linking was 95% pure (fig 2, lane PARN). The resulting chromatogram of the SEC- fractionation revealed four peaks eluting at 0.88 ml (fig 3A, P1), 1.33 ml (fig 3A, P2), 1.43 ml (fig 3A, P3) and 1.62 ml (fig 3A, P4). Peak P2 was eluted between the markers for ferritin (440 kDa) and aldolase (158 kDa). Peaks P3 and P4 were both fractionated between the size markers for aldolase (158 kDa) and ovalbumin (43 kDa). The estimated molecular weight of the peaks were P1~1800 kDa, P2 232 kDa, P3 147 kDa and for P4 64 kDa. Thus, it appears as if P1 corresponds to an aggregation of PARN polypeptides and that P4 corresponds to monomeric PARN while peaks P2 and P3 could correspond to oligomeric versions of PARN.

To investigate the potential oligomeric composition of the PARN polypeptides in peaks P1-P4 we performed cross-linking studies. Cross linking of un-fractionated PARN with BS^3 revealed three different cross-linked products, referred to as B2, B3 and B4,

respectively (fig 3B). Two cross-linked products B2 and B3 are of particular interest, since the product B3 has an estimated molecular weights of over 260 kDa (fig 3B, band B3) and the product B2 has an estimated molecular weight just above 135 kDa (fig 3B, band B2). The product designated B1 in figure 3B corresponds most likely to monomeric PARN since the estimated molecular weight of the band, 74 kDa, corresponds to the molecular weight of PARN and that the B1 band is not visible after cross-linking although it is present in the untreated sample. The first peak that appears around 0.88 ml in the chromatogram (fig. 3A) represents most likely an aggregation of PARN, which would then likely correspond to the upper band in the cross-linking assay (fig 3B, close to the stacking/separation gel interface). All the described products, B1-B4, contained PARN, as confirmed by Western blotting using antibodies against PARN as the probe (data not shown).

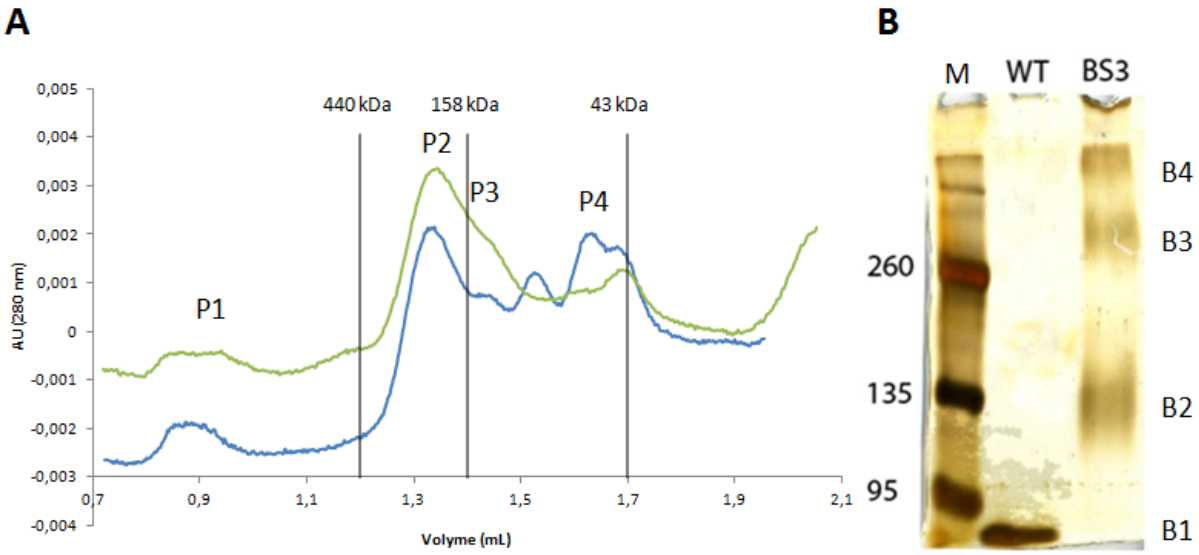

Figure 3. The oligomeric structure of PARN. A) Shows the UV 280 nm profile of the Superdex-200 gel-filtrated PARN fraction. The green and blue lines show fractionation of PARN in the presence of 50 mM KH_2PO_4/K_2HPO_4 pH 7.0 or 200 mM NaCl, respectively with a flow rate of 40 µl/min. Peak P2-P4 show different oligomers of PARN. Peak P2 was fractionated between the size markers for ferritin (440 kDa) and aldolase (158 kDa). Peak P3 and peak P4 were fractionated between the size markers for aldolase (158 kDa) and ovalbumin (43 kDa). The peak P2 corresponds in molecular size to a potential PARN tetramer with a molecular size of 296 kDa, whereas peaks P3 and P4 fractionate at molecular weights corresponding to dimers and monomers of PARN with molecular weights of 148 kDa or 74 kDa, respectively. The large size of peak P1 implies that it corresponds to a protein aggregate. B) Shows cross-linking of PARN, using 10 mM BS3 (lane BS3) during cross-linking. Band B3 mark the positions of potential PARN tetramer (lane BS3), B2 mark the position of the PARN dimer and band B1 shows the migration of untreated PARN (monomer). The cross-linked material was analyzed on a SDS-PAGE with a 5 % separation gel

Taken together these analyses imply that products B2 and B3 in fig 3B could correspond to a potential tetramer (*i.e.* B3) and dimer (*i.e.* B2) of PARN with molecular weights of 296 kDa and 148 kDa, respectively. These data imply that PARN may not only be present as a dimer but could also form larger oligomers, for example a tetramer. A tetrameric organization of PARN could potentially be established through a “dimer of dimers”

where each dimer is held together by the nuclease –nuclease domain dimerization interface and the "dimer of dimers" is held together by an RRM-RRM dimerization event.

3.3 Salt effects

The efficiency of deadenylation activity of native PARN depends on the 5' end structure of the mRNA substrate, i.e. whether the mRNA is capped (m7GpppG) or not (pppG). The in vitro deadenylation rate of capped mRNA substrate is approximately six fold faster than uncapped mRNA (Martínez et al., 2000, 2001). The cap stimulation in the deadenylase activity is reduced for recombinant PARN (Wu et al. 2008). The reduced cap stimulation for recombinant PARN could be due to several reasons, including post-translational modifications that will be absent from bacterially produced PARN. Another possible reason for the lower activity when using bacterially produced PARN could be due to a difference in the oligomeric composition of bacterially produced relative native PARN. In native PARN the oligomeric composition is predominantly larger than a dimer (Martinez et al., 2000), whereas the oligomeric composition of recombinant PARN is primarily dimeric and monomeric (see above and fig 3).

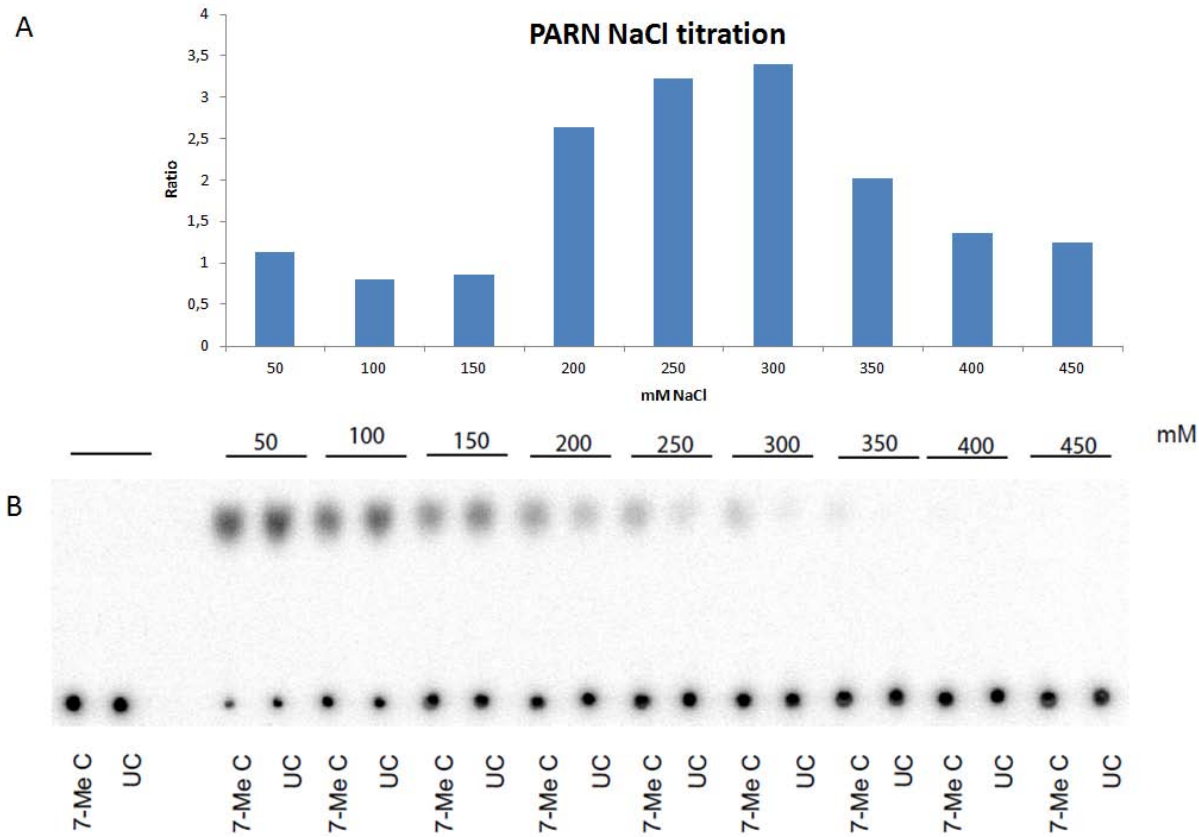

Figure 4. The effect on deadenylation activities of PARN in increasing NaCl concentrations. A) Shows the ratio between deadenylation activity by PARN on capped and uncapped mRNA substrates from the raw data in panel B. B) Show the result of the deadenylation assay on capped and uncapped mRNA substrates by 8 nM PARN, the negative control for each substrate without PARN are shown to the left.

To test if an experimental hydrophobic effect can be used to increase the amount of PARN tetramers when using recombinant PARN, we increased the monovalent ion concentration in deadenylation reactions. The potential hydrophobic effect induced by

salt was tested in *in vitro* deadenylation assays by increasing the NaCl concentration in reactions containing a fixed concentration PARN (8 nM). To be able to investigate the cap stimulation effect both capped and uncapped mRNA substrates were used and the release of the mononucleotide AMP was monitored (fig 4B).

At low NaCl concentration (50-150 mM NaCl) the cap stimulation was low (fig 4A), while a two to three fold cap stimulation effect was observed when the salt concentrations were between 200-300 mM NaCl (fig 4A). At very high ion concentration (350-450 mM NaCl) the deadenylation activity was very low (fig 4B). In general the deadenylation activity was increased when the ion concentration was increased (fig 4B).

The rationale behind this experiment was to increase oligomerization of PARN, which will be dependent on hydrophobic interactions, by increasing the salt concentration. Interestingly, high ion concentration induced the cap stimulated mRNA deadenylation activity of PARN. Thus, the "salt effect" can be used to increase the relative cap stimulation effect of PARN although high ion concentration decreased the overall deadenylation activity of PARN. To analyze the cap stimulation at high ion concentration a higher enzyme concentration might be necessary. One possible interpretation of this "salt effect" could be that the increased ion strength increased the hydrophobic interaction within the hydrophobic core and possibly also the protein-protein interactions of PARN (fig 4A). This will be in keeping with the proposal that the oligomeric state of PARN affects its cap-dependent activity.

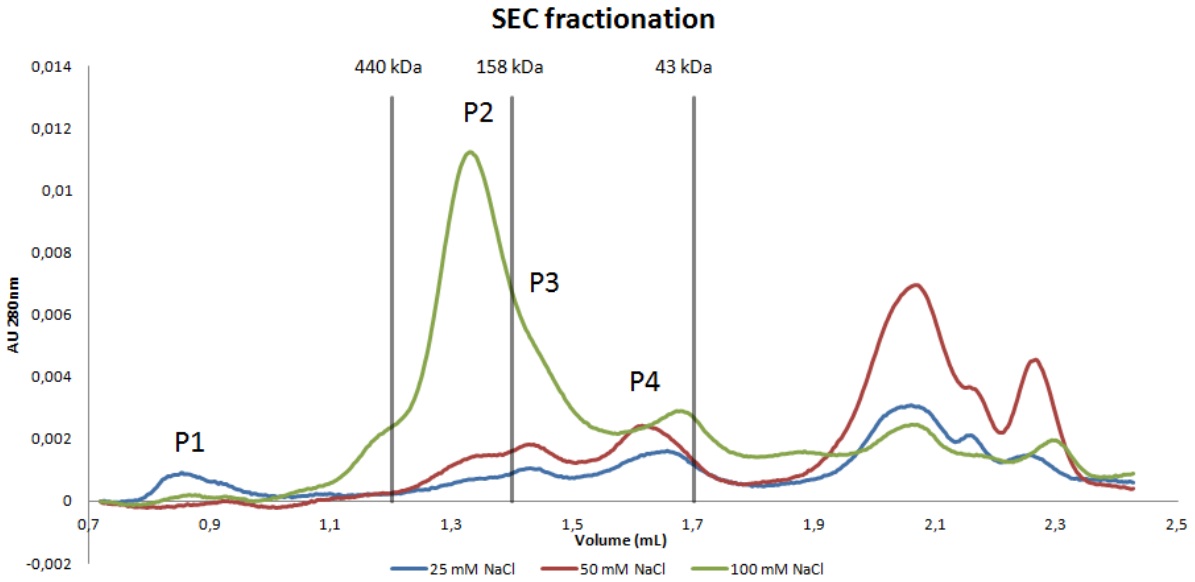

Figure 5. SEC-fractionation of PARN in 50 mM KH_2PO_4/K_2HPO_4 pH 7.0 and with different NaCl concentrations, 25 mM NaCl (blue), 50 mM NaCl (red) and 100 mM NaCl (green) with a flow rate of 40 µl/min. Peak P2 fractionates between the size markers (440 kDa) and aldolase (158 kDa) that corresponds to the estimated molecular weight of 232 kDa. Peaks P3 and P4 were fractionated between the aldolase (158 kDa) and ovalbumin (43 kDa). Peak P3 and P4 correspond to the molecular weights of 147 kDa and 64 kDa, respectively.

At high ion concentrations (200-300 mM NaCl) gave a significant cap stimulated deadenylation activity and we speculate that this effect was due to an increased protein-protein interaction. To investigate if changes in protein-protein interaction occurred

when the ion concentration was increased we utilized SEC-fractionation. To investigate if the addition of salt influenced the oligomeric structure of PARN we fractionated PARN by SEC at different monovalent ion concentrations. The resulting chromatograms are shown in figure 5.

When PARN was fractionated in presence of 25 mM or 50 mM NaCl the dominant peaks were peaks P3 and P4 (fig 5), that fractionated between the aldolase (158 kDa) and ovalbumin (43 kDa) size markers. Peak P3 and P4 were fractionated at 1.326 min and 1.604 min, which corresponded to molecular weights of 147 kDa and 64 kDa, respectively. When the salt concentration was increased to 100 mM NaCl we observed that the signal of peak P2, which fractionated between the size markers for ferritin (440 kDa) and aldolase (158 kDa), increased significantly (fig 5, peak P2). The estimated molecular weight of peak P2 was 236 kDa, which would correspond to a potential PARN tetramer.

At low salt concentration the hydrophobic effect is reduced and also the force that holds potential oligomers together. This analysis showed that the ion strength affected the SEC-fractionation pattern of PARN and implied that slat could modulate oligomerization of recombinant PARN. Most interestingly, when the ion concentration was increased we detected and increased cap stimulation effect (fig 4A), which correlated with the appearance of larger PARN oligomers (fig 5). Taken together, these experiments support the conclusion that cap stimulation originates from larger oligomers of PARN.

In the salt titration assay we also observed that the deadenylase activities were reduced at high ion concentration while the relative cap stimulation effect was reduced at low ion concentration. To further investigate the cap stimulation effect at a low ion concentration range we titrated the PARN concentration during *in vitro* deadenylation assays in the presence of 100 mM NaCl (fig 6A) or 200 mM NaCl (fig 6B).

At high PARN concentration, under both ion concentrations, the difference in deadenylation activity was small between capped and uncapped mRNA substrates. Thus, the cap stimulated activity was masked by the high deadenylation activity resulting from the use of high enzyme concentrations. However, a cap stimulated deadenylase activity was observed at low PARN concentration. When using 100 mM NaCl we observed cap stimulation when we used PARN concentration between 0.5-4 nM (fig 6A), while at 200 mM NaCl we observed cap stimulation between 4-8 nM PARN (fig 6B). As previously observed (fig. 4) the relative cap stimulation was, in comparison to reactions performed in the presence of 100 mM NaCl, increased in 200 mM NaCl.

The cap stimulation effect could be observed at a PARN concentration if the ion concentration was increased at the same time. This implies that the reduced cap stimulated deadenylation at low NaCl concentration (fig 4) was a result of high overall activity that shadowed the cap activity. In essence, the cap stimulation activity increases with an increased ion concentration. Thus, the monovalent ion concentration plays an important role for the possibility to detect the cap stimulatory effect on PARN.

To investigate if the cap stimulation activity correlates with the presence of larger PARN oligomers we performed *in vitro* deadenylation activity assays using the collected peak fractions, presented by the green chromatogram in fig 3,. The deadenylation reactions were performed in 200 mM NaCl to stimulate the cap activity (fig 6C).

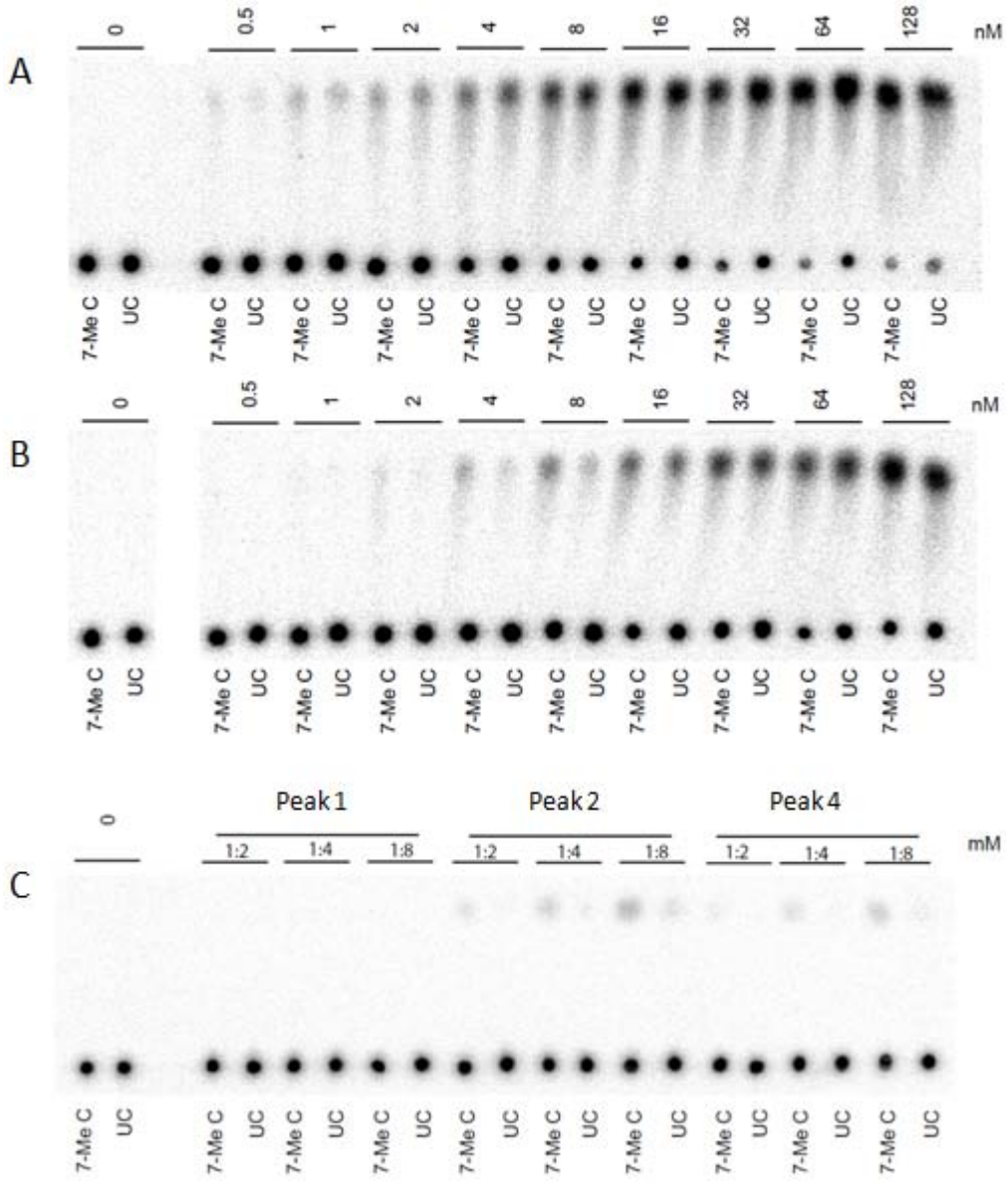

Figure 6. Deadenylation activities *in vitro* on capped and uncapped L3(A_{30}) mRNA substrate of PARN titrations. In A) 100 mM NaCl and in B) and C 200 mM NaCl was used in the reaction assay. In A and B PARN was titrated from 0-128 nM with capped (7-Me C) and uncapped (UC) L3(A_{30}) substrate. C) Shows the deadenylation of SEC-fractionated PARN from fig 1A (blue chromatogram) on capped and uncapped L3(A_{30}). Peak 1, 2 and 4 was tested for deadenylase activity. The peak fractions were diluted 2-8 times. For all titrations 5'-AMP release was analyzed.

The relative cap stimulation activity was increased when PARN was diluted and the maximum cap stimulation activity was obtained when the peak fraction was diluted eight times (fig 6C). This behavior might be due to local aggregation of PARN in the high salt concentration. The first collected peak P1 had no activity (fig 6C, peak P1). The other two collected peaks P2 and P4 revealed high activity for capped substrate (fig 6C, peak P2 and P4). Peak P2 had the highest activity with capped substrate and peak P4 had lower cap activity (fig 6C).

The cap stimulation was highest when using PARN that was fractionated in peak P2, which we have assigned to be a likely tetramer of PARN. We also observed high cap stimulation when using PARN that fractionated in peak P4, which we have assigned to be the PARN monomer. The cap activity is peak P4 was unexpected since our working model proposes that the cap stimulation effect correlates with the presence of PARN tetramer. The high cap activity detected when using PARN fractionated in peak P4 could be explained by the possibility that the high salt concentration used during the deadenylation reaction reformed the tetramer. Further experiments are required to unambiguously conclude that the higher cap effect observed at 200-300 mM NaCl is due to oligomerization effects of PARN.

3.4 RRM dimeric model

The RRM of PARN contributes to three essential properties of PARN; substrate binding (Nilsson et al., 2007), cap interaction (Nilsson et al., 2007 and Wu et al., 2009) and RRM dimerization (Niedzwiecka et al., 2011). All these functions require amino acid residues located within the RRM. A functional RRM dimerization surface requires that a combination of structural and functional conditions are fulfilled; *i*) the surface should preferentially not interfere with cap or substrate binding, *ii*) be large enough to form a stable interaction surface between the two RRM subunits, and *iii*) the RRM dimerization surface has to be placed so it is in accordance with the dimeric PARN structure that is stabilized by the nuclease domain interaction.

In the structure of dimeric PARN the RRMs are located on the opposite sides of the nuclease dimer (fig 7A). RRM dimerization is therefore unlikely within a PARN dimer unless there is a major conformational change of the PARN dimer. However, in a tetrameric organization based on a “dimer of dimers”, the RRMs of two independent dimers could potentially be placed in close vicinity of each other. Figure 7A shows the open and closed conformation of PARN and a potential dimerization surface is observed in each RRM (encircled region in fig 7A, B and C). If the entire PARN dimer in fig 7A is rotated 90˚ counter clockwise the RRMs will appear on the same side of the PARN dimer whereas the R3Hs will be on the opposite side (fig 7B). In this orientation a potential dimerization surface of the RRM (fig 7C) that fulfills all the requirements, as outlined above, can be identified. The potential surface is sufficiently large, contains hydrophobic amino acids that could interact with each other and the surface will not mask the cap-binding site, including Trp-475 and amino acids its vicinity, or the RNA binding site of the RRM, which is most likely located on the β-pleated sheet surface of the RRM. And significantly, the RRMs of two independent dimers can be placed in close vicinity of each other if a tetrameric conformation is envisioned.

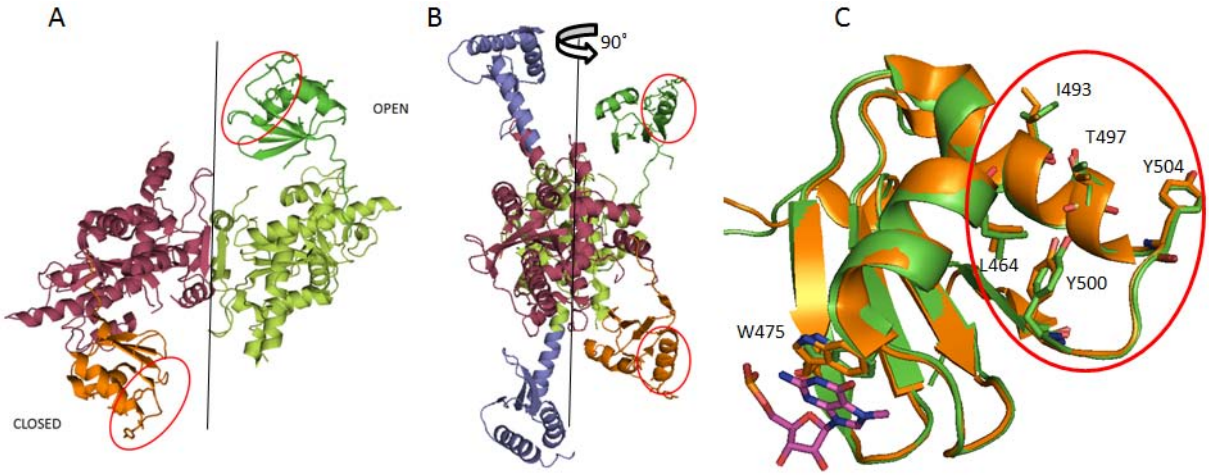

Figure 7. In A the crystal structure of pdb: 3D45 that shows the dimer of PARN with dimerization between the nuclease domains (purple and light green) and the location of two RRMs, dark green (open) and orange (closed), the red circles shows the location of the proposed RRM-RRM dimer interaction patch. B is the model of the structure pdb: 3D45 aligned to 2A1S. B is a 90° clockwise rotation of A, the R3H domains are in dark blue. C the structural alignment of the open and closed RRM structure shows the location where the cap interacts with the RRM and the proposed dimerization patch (red circle).

To identify amino acids that may participate in dimerization a structural alignment was made between the opened and closed RRM. The difference in structure between the open and closed conformation of the RRM is small. The following amino acids were identified as candidates to be involved in the dimerization of the RRM, Leu-464, Ile-493, Thr-497, Tyr-500 and Tyr-504 (fig 7C, encircled).

In the RRM dimerization model stacking is possible between the tyrosines from each RRM, Tyr-500 RRM_1 stacks with Tyr-504 RRM_2 and Tyr-504 RRM_1 stacks with Tyr-500 RRM_2. The tyrosine stacking provides specificity for the RRM-RRM interaction. The RRM in the modeled dimer has opposing direction. The amino acids Leu-464, Ile-493 and Thr-497 stabilize the predicted dimerization interaction. Amino acid residues Leu-464, Ile-493 and Tyr-500 are potentially involved in creating a hydrophobic core of the RRM dimer, indicating that the RRM dimerization is built around a common hydrophobic core that also will reduce the exposure of hydrophobic amino acids on the surface of each monomeric RRM subunit.

3.5 Verifying the RRM dimeric model

The model implies that amino acids Leu-464, Ile-493, Thr-497, Tyr-500 and Tyr-504 participate in RRM dimer formation. To test the model the identified candidate amino acids were mutated to alanine residues. The effect the mutants had on tetramerization was subsequently analyzed with BS^3 cross-linking.

BS3 cross-linking data showed that none of the introduced single alanine substitutions in the RRM abolished PARN tetramerization (fig 8, lanes 4, 6, 8, 10 and 12). Therefore we investigated if double mutations in the RRM would interfere with PARN tetramerization. To the single mutant L464A a second round of single alanine substitution was introduced at the positions Ile-493, Thr-497, Tyr-500 and Tyr-504. The double mutation with Ile-493 and Thr-497 behaved as PARN and the introduced mutations had no effect tetramerization (fig 8, lanes 14 and 16). However, in the double mutants L464A Y500A and L464A Y504A the tetramer band appeared as a smear and no distinct tetramer band could be visualized (fig 8, lane 18 and 20).

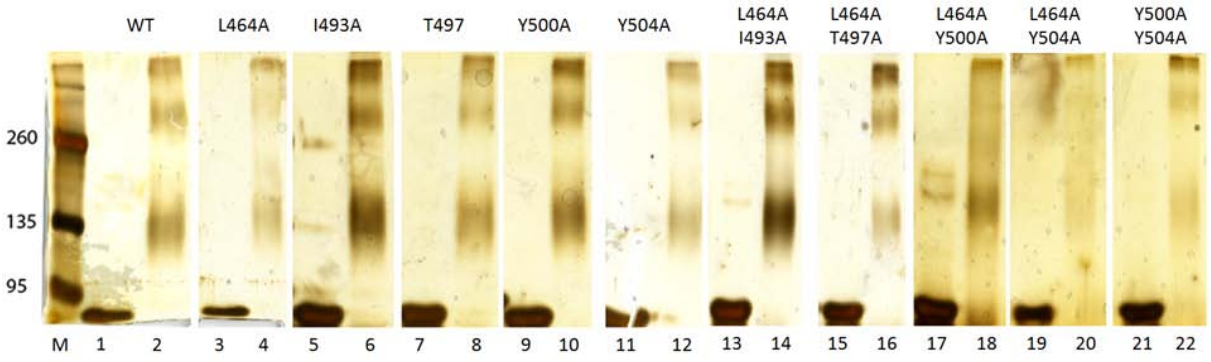

Figure 8. Cross-linking of PARN with alanine mutations at the proposed tetramerization position in the RRM, odd number lanes contains the uncross-linked PARN and mutants. Even numbered lanes was PARN and mutations cross-linked with 10 mM BS^3.

The tyrosines Y500 and Y504 are potentially involved in tyrosine stacking during RRM dimerization and a double mutant Y500, 504A could potentially affect PARN tetramerization. However, the double tyrosine mutant Y500, 504A had the same cross-linking pattern as wt PARN (fig 8, lane 22).

One explanation why RRM dimerization was not affected in the Y500, 504A mutant could be that the introduction of hydrophobic alanine residues actually strengthens the hydrophobic core of the RRM interaction surface and thereby does not affect the PARN tetramerization. The introduction of charged amino acids or glycine residues would experimentally address this possibility. We also tested the effect the mutations of the two tyrosine residues had on the PARN deadenylation activity. However, we were not able to detect any significant changes in cap stimulation that was caused by mutating the two tyrosine residues 500 and 504 (fig 9).

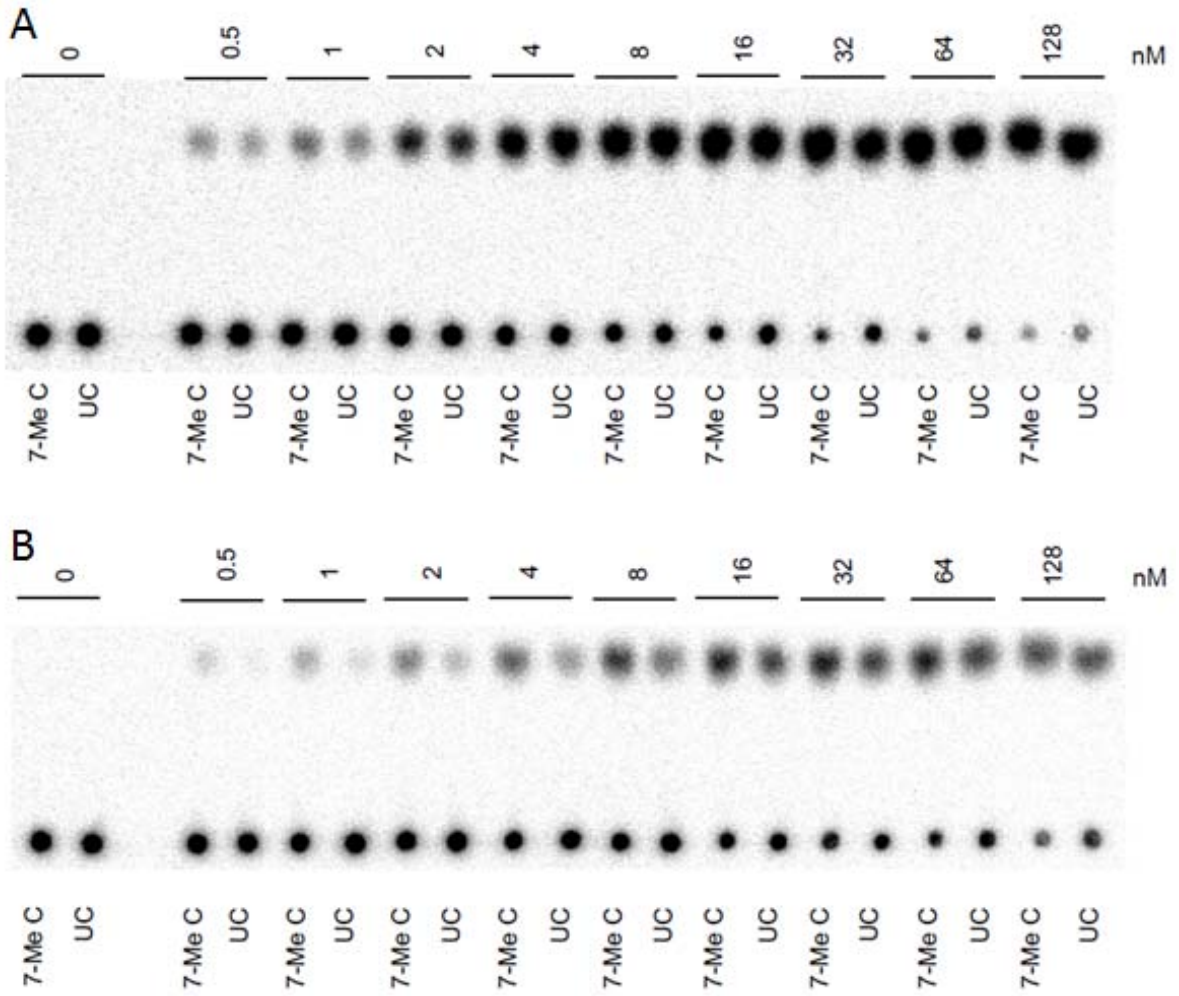

Figure 9. Deadenylation activities of the double tyrosine PARN mutant (Y500A and Y504A) on capped and uncapped L3(A_{30}) mRNA substrate and analysis of 5'-AMP release. The *in vitro* deadenylation reaction was performed in A) 100 mM NaCl and B) 200 mM NaCl.

4 Discussion

The SEC-analysis shows that PARN can be fractionated into different size classes, which we assume represent tetramers, dimers and monomers, respectively (fig 6C). The salt titration both in SEC-fractionation and deadenylation showed that the recombinant PARN formed larger complexes in higher ion concentrations. The SEC-filtration showed that a potential tetramer was the highest oligomeric state of PARN to have deadenylation activity and that cap stimulated deadenylation activity could be due to tetramerization of PARN. Efficient oligomerization was dependent on the ion concentration (fig 5). The ion strength dependency of PARN oligomerization shows that the ion concentration is paramount in studies of PARN activity.

To perform a study with a recombinant protein is fast and straight forward; the protein is produced in *E.coli* and easily purified. In the case of PARN we have activity data from native PARN to compare with. Native PARN has a six fold higher deadenylation activity on capped mRNA substrate as compared to the uncapped counterpart (Martínez et al., 2000). Native PARN also has an oligomeric structure (Martínez et al., 2000). In native PARN the oligomeric arrangement could very well be homogenously tetrameric whereas in recombinant PARN the oligomeric arrangement appears to be distributed over a large range of oligomeric states. One of the major shortcomings of recombinant PARN has been the low cap stimulation effect on mRNA deadenylation. It has previously been observed that the cap stimulation can be regained when using recombinant PARN if the buffer is changed to a potassium phosphate based buffer instead of the commonly used Tris-based buffer (Wu et al., 2009). In this study we have preliminarily found that the cap stimulatory deadenylation correlates with the oligomeric state of PARN. And that the oligomeric state could be modulated by changing the ion conditions of deadenylation reactions. We also observed that high ionic strength increased the cap stimulatory activity although high salt conditions at the same time decreased the overall deadenylation activity.

In the current working model of PARN it has been proposed that the RRM of one monomer of dimeric PARN, through its movement, pushes the poly(A) substrate into the active site (Henriksson et al., 2010). While the other monomer holds the 5' end located cap structure. A key question is therefore how the cap structure can, across the PARN dimer and at long distance, stimulate deadenylation at the hydrolytic site in the other monomer.

Based on the data obtained in this study we propose a model for tetrameric deadenylation by PARN, which could explain how the cap bound in one active site of PARN, stimulates the hydrolytic reaction in the other active site. The key proposals are that two RRMs originating from two different dimers of PARN dimerize and come in close proximity to each other in a tetrameric model of PARN and that the nearness, i.e. dimerization, will allow molecular communication between the two active sites, one site being hydrolytically active whereas the other site will act as the allosteric cap binding site. It is worthwhile to mention that RRM/RRM dimerization is not likely in a dimeric

model of PARN. Figure 10 shows a schematic drawing of tetrameric PARN. In this figure the tetrameric deadenylation process is schematically shown as three steps (fig 10). In the beginning the site for hydrolysis is empty and to fill this position the RRM close to the hydrolytic site begins to rotate toward the nuclease domain and the RRM goes from open to closed conformation. This movement drives the rotation of the RRM at the cap binding site from closed conformation to open. The rotation of the cap RRM pulls the first transcribed nucleotide residue (indicated as a G residue in the figure) out from the active site. At the hydrolytic site the poly(A) substrate is pushed by the RRM into the active site for hydrolysis (fig 10, compare panels A and B). When the RRM at the active site has come to the fully closed position, all the adenosine binding positions in the active site have become filled with adenine residues. Hydrolysis occurs and then the RRM at the hydrolytic site begins to rotate back to the open conformation (fig 10, compare panels B and C). We propose that the rotation back of the RRM at the active site is driven by the simultaneous movement of the RRM at the cap binding site, which will push the first transcribed guanine back into the active site.. In the next round of hydrolysis the movement of the RRM at the active site of hydrolysis will push, i.e. translocate, in the poly(A) substrate again into the hydrolytic position, which at the same time will push out the released AMP product (colored in red in the figure) out from the active site. This model provides a reasonable explanation for how the cap and how stimulates PARN mediated deadenylation. In short, the counter actions of the RRM dimer always force one of the RRM to be in the unfavorable open position and the fight between them is what drives the feeding of the substrate into the active site. This also explains why the reaction is slower without the cap, without the cap the there is no counterpart to balance the reaction and the conformational change of the RRM becomes slower.

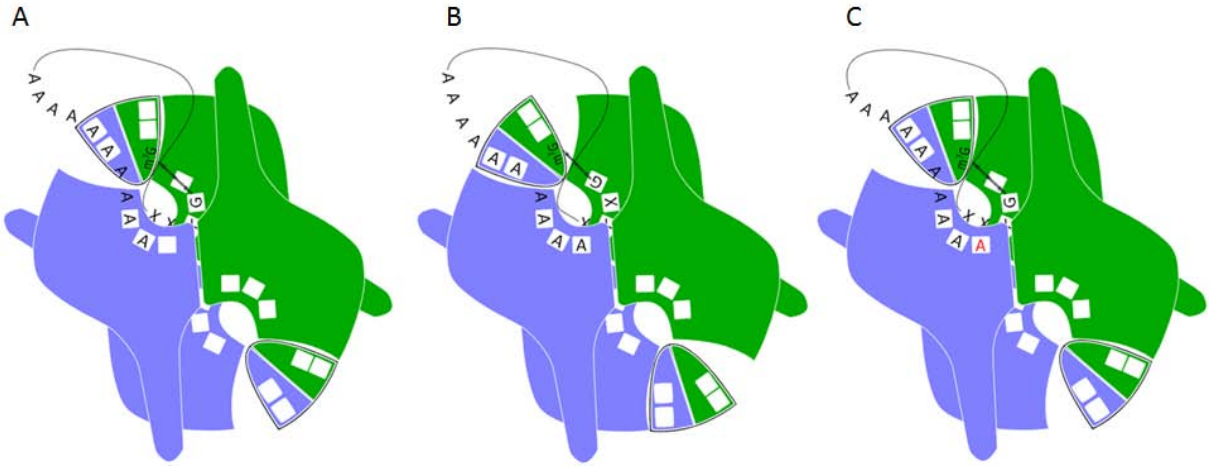

Figure 10. The tetrameric model of deadenylation of PARN. A-C describes the rotation of the RRM dimer, the movement of the substrate and the influence of the 5'-cap structure.

Taken together, we have presented a mechanistic model for PARN mediated deadenylation based on a tetrameric conformation of PARN. We have obtained preliminary evidence that PARN can form tetramers but we have not yet been able to identify a suitable mutation that prevents PARN tetramerization.

5 References

Balatsos NA, Nilsson P, Mazza C, Cusack S, Virtanen A., 2005 Inhibition of mRNA deadenylation by the nuclear cap binding complex (CBC). J Biol Chem. 281(7):4517-22.

Cevher MA, Zhang X, Fernandez S, Kim S, Baquero J, Nilsson P, Lee S, Virtanen A, Kleiman FE., 2010 Nuclear deadenylation/polyadenylation factors regulate 3' processing in response to DNA damage. EMBO J. 29(10):1674-87.

Denis CL, Chen J., 2003 The CCR4-NOT complex plays diverse roles in mRNA metabolism. Prog Nucleic Acid Res Mol Biol. 73:221-50.

Gao M, Fritz DT, Ford LP, Wilusz J., 2000 Interaction between a poly(A)-specific ribonuclease and the 5' cap influences mRNA deadenylation rates *in vitro*. Mol Cell. 5(3):479-88.

Garneau NL, Wilusz J, Wilusz CJ., 2007 The highways and byways of mRNA decay. Nat Rev Mol Cell Biol. 8(2):113-26.

Goldstrohm AC, Wickens M., 2008 Multifunctional deadenylase complexes diversify mRNA control. Nat Rev Mol Cell Biol. 9(4):337-44.

Gorgoni B, Gray NK., 2004 The roles of cytoplasmic poly(A)-binding proteins in regulating gene expression: a developmental perspective. Brief Funct Genomic Proteomic. 3(2):125-41.

Halbeisen RE, Galgano A, Scherrer T, Gerber AP., 2008 Post-transcriptional gene regulation: from genome-wide studies to principles. Cell Mol Life Sci.65(5):798-813.

Henriksson N, Nilsson P, Wu M, Song H, Virtanen A., 2010 Recognition of adenosine residues by the active site of poly(A)-specific ribonuclease. J Biol Chem. 285(1):163-70.

Liu WF, Zhang A, Cheng Y, Zhou HM, Yan YB.,2009 Allosteric regulation of human poly(A)-specific ribonuclease by cap and potassium ions. Biochem Biophys Res Commun. 379(2):341-5.

Liu WF, Zhang A, He GJ, Yan YB., 2007 The R3H domain stabilizes poly(A)-specific ribonuclease by stabilizing the RRM domain. Biochem Biophys Res Commun. 360(4):846-51.

Mandel CR, Bai Y, Tong L., 2008 Protein factors in pre-mRNA 3'-end processing. Cell Mol Life Sci. 65(7-8):1099-122.

Martinez J, Ren YG, Thuresson AC, Hellman U, Astrom J, Virtanen A., 2000 A 54-kDa fragment of the Poly(A)-specific ribonuclease is an oligomeric, processive, and cap-interacting Poly(A)-specific 3' exonuclease. J Biol Chem. 275(31):24222-30.

Martînez J, Ren YG, Nilsson P, Ehrenberg M, Virtanen A., 2001 The mRNA cap structure stimulates rate of poly(A) removal and amplifies processivity of degradation. J Biol Chem. 276(30):27923-9.

Nilsson P, Virtanen A., 2006 Expression and purification of recombinant poly(A)-specific ribonuclease (PARN). Int J Biol Macromol. 39(1-3):95-9.

Nilsson P, Henriksson N, Niedzwiecka A, Balatsos NA, Kokkoris K, Eriksson J, Virtanen A., 2007 A multifunctional RNA recognition motif in poly(A)-specific ribonuclease with cap and poly(A) binding properties. J Biol Chem. 282(45):32902-11.

Parker R, Song H., 2004 The enzymes and control of eukaryotic mRNA turnover. Nat Struct Mol Biol. 11(2):121-7.

Proudfoot NJ, Furger A, Dye MJ., 2002 Integrating mRNA processing with transcription. Cell 22;108(4):501-12.

Ren YG, Martínez J, Virtanen A., 2002 Identification of the active site of poly(A)-specific ribonuclease by site-directed mutagenesis and Fe(2+)-mediated cleavage. J Biol Chem. 277(8):5982-7.

Ren YG, Kirsebom LA, Virtanen A., 2004 Coordination of divalent metal ions in the active site of poly(A)-specific ribonuclease. J Biol Chem. 279(47):48702-6.

Tang G., 2005 siRNA and miRNA: an insight into RISCs. Trends Biochem Sci. 30(2):106-14.

Zhang X, Virtanen A, Kleiman FE., 2010 To polyadenylate or to deadenylate: that is the question. Cell Cycle. 2010 9(22):4437-49.

Wu M, Reuter M, Lilie H, Liu Y, Wahle E, Song H., 2005 Structural insight into poly(A) binding and catalytic mechanism of human PARN. EMBO J. 24(23):4082-93.

Wu M, Nilsson P, Henriksson N, Niedzwiecka A, Lim MK, Cheng Z, Kokkoris K, Virtanen A, Song H., 2009 Structural basis of m(7)GpppG binding to poly(A)-specific ribonuclease. Structure 17(2):276-86.

Åström J, Åström A, Virtanen A., 1992 Properties of a HeLa cell 3' exonuclease specific for degrading poly(A) tails of mammalian mRNA. J Biol Chem. 267(25):18154-9.